SURFACE RESISTANCE STUDY ON LOW FREQUENCY (LOW BETA) CAVITIES

D. Longuevergne, F. Chatelet, G. Michel, G. Olry, F. Rabehasy, L. Renard, IPNO, Orsay, France

Abstract

Additional RF tests and temperature treatments (120°C baking, 100K soaking, ...) have been carried out on Spiral2 quarter-wave resonator (QWR) and ESS double spoke resonator (DSR). For each test, residual resistance and BCS resistance have been evaluated by testing the cavities between 4.2K and 1.5K. This talk will summarize the main results and try to highlight the main differences with high frequency cavities.

INTRODUCTION

The analysis of the evolution of the quality factor (noted Q_0) versus the accelerating gradient (noted Eacc) of a superconducting cavity made of bulk Niobium has been in the community very important and fruitful to optimize the surface and heat treatments. This way, three regions of importance have been defined based on general observation of 1.3 GHz elliptical cavities; the Low, Medium and High Field Q-Slope, noted respectively LFQS, MFQS and HFQS. LFQS corresponds to a slight increase of the Q_0, the MFQS to a slow decrease of the Q_0 and finally the HFQS to a fast decrease of the Q_0 [1].

It has to be pointed out that this general behaviour has never been observed at lower frequencies (88 MHz and 352 MHz); the Q-slope is monotonous, progressive and starts already at low field (see Figure 1).
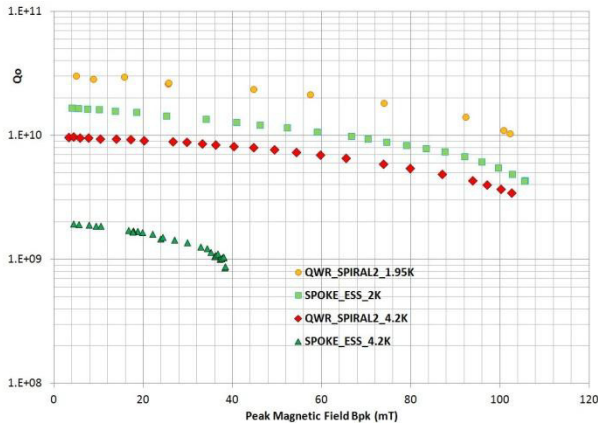

Figure 1: Typical Q-curve of Spiral2 QWR and ESS DSR.

The aim of this paper is to report some typical behaviour of cavities operating at 88 MHz (Spiral2 QWR) and 352 MHz (ESS DSR).

Extensive cold tests between 4.2K and 1.5K in vertical cryostat have been carried out to fully understand the evolution of the residual and BCS resistance (noted R_{res} and R_{BCS}) versus Eacc. By quantifying both the residual and BCS resistances of the cavity versus the accelerating gradient, one can fully assess what is the best procedure to treat the surface of a cavity regarding the specifications of a project. The advantage is that at these low frequencies and at 2K, R_{BCS} is small and even negligible at 88 MHz contrary to 1.3 GHz cavities where R_{BCS} stays comparable to R_{res}. Table 1 summarizes typical values of R_{BCS}.

In order to extract correctly both resistances and their dependences versus Eacc, an empirical model has been built as described in [2], based on the magnetic dependence of the energy gap for R_{BCS}. The field dependence of R_{res} is fitted with a second order polynomial function because of its complexity. It appears that this model is fitting very nicely the Q-slope visible on experimental data at 88 MHz. However, at 352 Mhz, the model can't be used due to a bad cooling of the cavity at 4.2K tested vertically instead of horizontally.

Table 1: Typical BCS Resistance Values Versus Frequency at Different Temperatures

R_{BCS} (nΩ)	4.2K	2K	1.5K
1300 MHz	600	15	1.2
700 MHz	174	4.3	0.35
352 MHz	44	1	9E-2
88 MHz	3	7E-2	6E-3

Finally, the magnetic ambiance around the cavity during cooling down has been monitored. Very interesting but complex behaviour has been observed without surprisingly any consequences on the quality factor of the cavities. Details will be given in this paper.

RS MODEL

The model used to interpret the R_{BCS} increase versus the amplitude of the RF magnetic field is based on the magnetic dependence of the energy gap as detailed in [2]. In other terms, the energy gap, difference of free energies between the normal and superconducting states, is altered by the magnetic energy brought by the RF wave.

We can write the corrected formula of the BCS resistance as in equation 1 :

$$R_{BCS} = \frac{A(\lambda, \xi, l, ...) \cdot \omega^2}{T} \cdot \exp\left(\frac{-\Delta(T=0, B=0)}{k_B \cdot T} \cdot \left(1 - \left(\beta \cdot \frac{B}{Bc(T)} \right)^2 \right) \right) \tag{1}$$

With A and β two parameters, T the temperature, ω the pulsation of the RF wave, Δ the energy gap, k_B the Boltzmann constant, B the amplitude of the RF magnetic field and Bc the critical magnetic field.

The other contribution to surface resistance, R_{res}, for which no particular model has been developed; is fitted by a simple 2nd order polynomial function (Eq. 2) as what has been commonly done in previous studies [3] and [4].

$$R_{res}(T,B) = R_{res0} \cdot \left(1 + \alpha \cdot \frac{B}{Bc(T)} + \left(\gamma \cdot \frac{B}{Bc(T)} \right)^2 \right) \quad (2)$$

We however consider the γ parameter as part of the residual contribution and not of BCS resistance because it remains at 2K, temperature at which the BCS resistance is negligible.

As detailed in [2], applying this model to fit Q_0 curves requires a correction of the famous formula $Q_0=G/Rs$. Indeed in this formula, the assumption is made that the surface resistance does not depend on magnetic field. That's not true anymore, leading to the following corrected formula (Eq. 3):

$$Q_0 = G \cdot \frac{\sum_i^n B_i^2 \cdot S_i}{\sum_i^n Rs_i(B_i) \cdot B_i^2 \cdot S_i} \quad (3)$$

With G the geometrical factor, B_i, Rs_i and S_i respectively the magnetic field, the surface resistance and the surface area exposed to a field between B_i and B_{i+1}. S_i are calculated and exported thanks to CST Microwave Studio. The RF surface is divided into n zones.
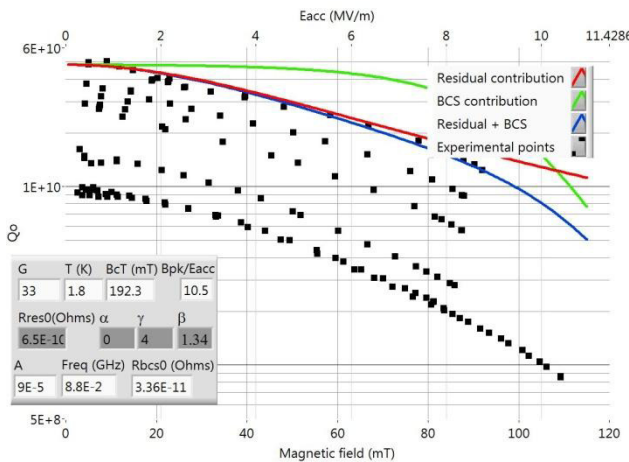
Figure 2 and 3 are showing two examples of fitting.

Figure 2: Fit of experimental results at 1.8K of an unbaked Spiral2 QWR. Black dots are the experimental data at several temperatures (from top to bottom: 1.8K, 2.25K, 2.7K, 3.5K and 4.2K), the green curve is giving the BCS contribution to the Q-slope, the red one the residual contribution to the Q-slope and the blue one the sum of both contributions.
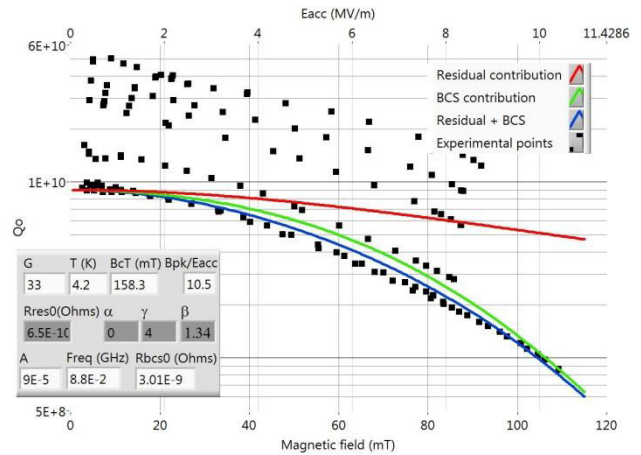

Figure 3: Fit of experimental results at 4.2K of the same cavity with the same fitting parameters. Only the temperature and thus Bc have been changed.

SPIRAL2 QWR RESULTS

These cavities are made of RRR=250 bulk Niobium and are operating at 88 MHz at a temperature of 4.2K [5]. The standard procedure to prepare them is first an ultrasonic degreasing, a deep BCP etching of at least 150 µm and a 48h 120°C baking under vacuum. It has been shown that the baking divided by two the power dissipation of the cavity at the operating gradient of 6.5 MV/m. A heat gun blows 120°C compressed air into the helium tank down to the bottom of the inner conductor. Heaters are stuck on the cavity bottom to help heating up as the helium tank doesn't extend down to the cavity bottom.

Analysis of Cavity Results

As depicted on Figure 4, we can see that the Q_0 of a baked cavity is higher at 4.2K but is lower below 2K. This proves that a 120°C baking is increasing the residual resistance but is decreasing the BCS resistance in accordance with [6].
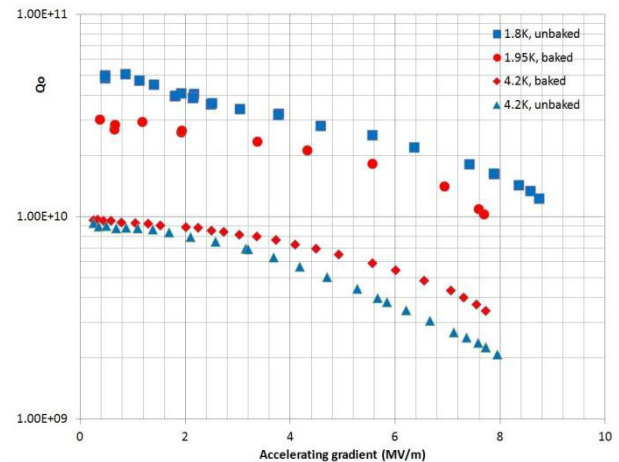

Figure 4: Spiral2 QWR tested before and after baking.

As a matter of fact, we can say that baking a cavity at this low frequency is justified if the cavity is operated at 4.2K but would degrade cavity performances if operated at 2K.

If we go farther in the analysis of fitting parameters (table 2), we can see that effectively, the BCS resistance has been improved of 27% whereas the residual resistance has been increased of 70%. The reduction of the BCS resistance is coming from the drop of the parameter A, taking into account several parameters of the material as the London penetration depth, coherence length and electron mean free path. Previous studies done at Saclay [7] showed that the reduction of BCS resistance is caused by a reduction of the electron mean free path toward the optimum value of about 20 nm [8] certainly due to the diffusion of impurities from the surface to the bulk material. The factor β has shown no changes before and after baking. We will see in next section that this parameter doesn't depend on the material but on the geometry. The increase of the residual resistance is significant whereas its quadratic magnetic field dependence parameterized by γ is divided by almost a factor of 1.4. The aim of this paper is not to focus on this γ parameter but the comprehension of its origin would be of great interest to improve cavity performances as the MFQS is dominated at 2K by the factor Rres*γ² before and after baking. (red curves of Figures 2 and 5 representing the residual contribution).
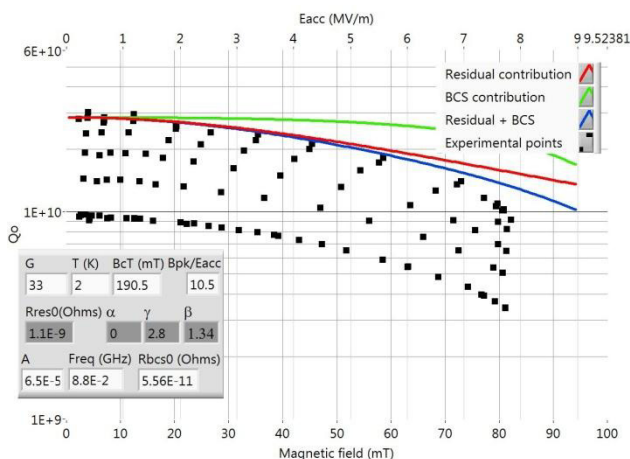

Figure 5: Fit of experimental results at 2K of a baked Spiral2 QWR. Black dots are the experimental data at several temperatures (from top to bottom: 2K, 2.5K, 3K, 3.5K and 4.2K), the green curve is giving the BCS contribution to the Q-slope, the red one the residual contribution to the Q-slope and the blue one the sum of both contributions. This cavity had X-rays emission after baking

RF Simulations and Peak Magnetic Field

Several Spiral2 QWR results have been fitted with the model presented previously. For each cavity, a different β parameter had to be defined typically between 1.3 and 1.7 considering a Bpk/Eacc of 10.5 mT/(MV/m). This spread

couldn't be explained by considering the β parameter as a reduction factor of the theoretical critical magnetic field Bc linked to Niobium quality as all cavities have been prepared following the same procedure with Niobium coming from the same supplier. The β factor could thus only be an enhancement factor of the surface magnetic field.

Table 2: Value of Resistances and Model Parameters Before and After Baking

	Unbaked cavity	**Baked cavity**
R_{BCS} at B=0 at 4.2K	3.01 nΩ	2.2 nΩ
R_{BCS} at B=0 below 2K	< 0.1 nΩ	< 0.1 nΩ
A	9E-5	6.5E-5
β	1.34	1.34
Rres at B=0	0.65 nΩ	1.1 nΩ
α	0	0
γ	4	2.8
Rres*γ² (nΩ)	10.4	8.6

A quench detection campaign [9] helped us localizing the problem that could explain the spread of the β factor. The quench was located on several cavities in the region of the welding between the cavity donut and the plunger port as showed with the red arrow on Figure 6. If the radius of curvature in this area was 5 mm as defined during the RF design study, the quench couldn't be located in this area but in the inner conductor (stem). The conclusion of this is that the radius of curvature in this area has not been controlled and would be between 1 and 2 mm. The graphic on Figure 6 depicts simulation results of the Bpk/Eacc factor (and thus the β factor) versus the radius of curvature in this region.
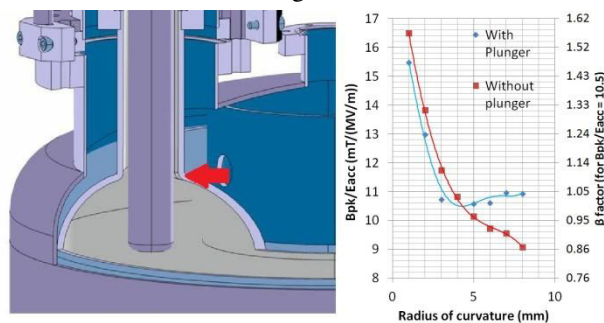

Figure 6: (left) Location of quench detected on a cavity without plunger. The theoretical radius of curvature is 5 mm. (right)

As a consequence, the real Bpk/Eacc of Spiral2 QWR is not 10.5 mT/(MV/m) but would be between 13 and 17 mT/(MV/m) explaining also why none of Spiral2 QWR would reach the theoretical limit Bc of 160 mT at 4.2K.

Another interesting observation, as shown on Figure 6, is that a cavity equipped with its tuning system (plunger) would quench at a higher accelerating gradient than without it as the Bpk/Eacc factor is lowered of about 1 mT/(MV/m) for a radius of curvature below 3 mm. This is well illustrated in Figures 2 and 3, as we can see that the Q_0 curve at 4.2K is extending up to 110 mT (test done in 2007 with a plunger) whereas all other tests at lower temperature and all Q_0 curves on Figure 5 are limited below 85 mT (tests done this year without plunger).

As a conclusion, the β factor of the surface resistance model is an adjustment factor of the theoretical Bpk/Eacc to the real one and is not a factor reflecting the quality of Niobium used.

Magnetic Behaviour During Cooling-Down

Since 2013, cryogenic magnetic sensors (fluxgate sensors) are routinely installed around the cavity to monitor the magnetic ambiance during cooling down as shown on Figure 7. Huge magnetic variations greater than 1000 mG have been observed on the bottom of the cavity (Figures 8 and 9) during cooling down without surprisingly impacting the performance of Spiral2 QWR (as shown in Figures 2 and 5).
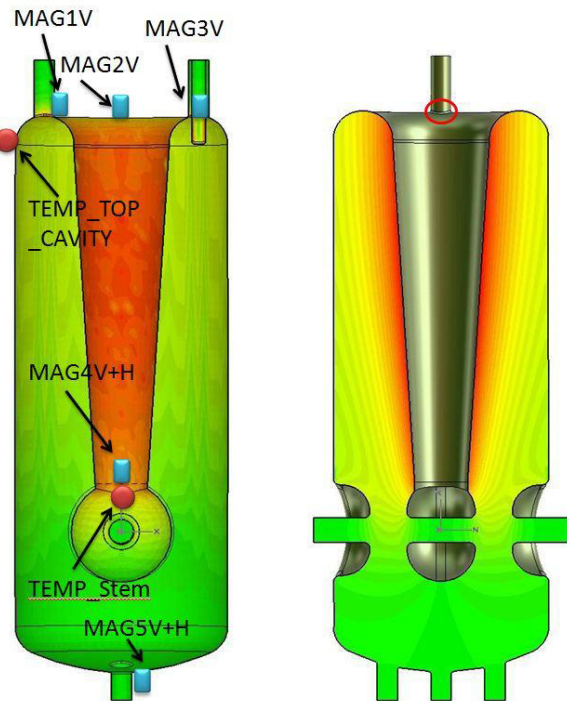

Figure 7: Distribution of RF magnetic field in a Spiral2 QWR. Position of magnetic (blue rectangle) and temperature (red circle) sensors during cavity testing. V and H in magnetic sensor names correspond to the component the magnetic probe are sensing respectively vertical and horizontal components. MAG1V and MAG3V and MAG5V are in contact with the cavity whereas MAG2V, MAG4V+H and MAG5H are not. The red circle gives the location of the quench detected as explained in previous section.
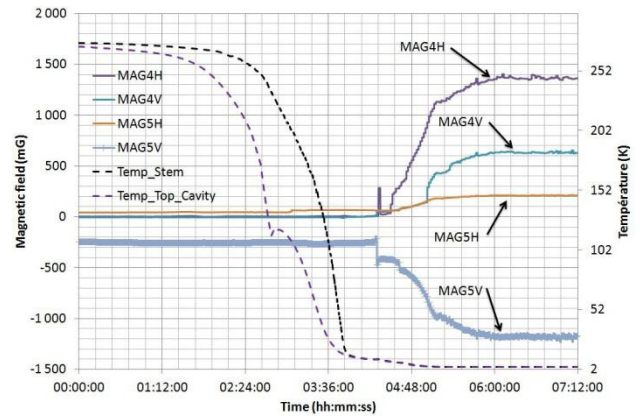

Figure 8: Evolution of the vertical and horizontal magnetic fields measured at the bottom of the inner conductor and the cavity during cooling down of a Spiral2 QWR. The significant magnetic field measured remain during the RF test and disappear when the cavity is warmed and reach around 50K.
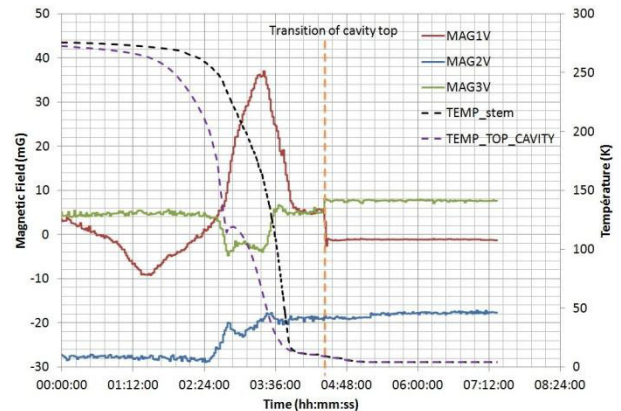

Figure 9: Evolution of the vertical magnetic field measured at the top of the inner conductor and the cavity during cooling down of a Spiral2 QWR. We can see clearly the magnetic field created by thermal currents especially on MAG1V sensor. The magnetic fields are then stabilizing when the thermal gradients are low. Finally a sharp transition is visible on MAG1V and MAG3V at a temperature around 9.2K.

Magnetic Sensitivity of Spiral2 QWR

Coils installed inside the warm magnetic shield of the cryostat allowed us to test the vertical magnetic sensitivity of cavities. The Spiral2 QWR sensitivity to vertical magnetic field is only of 0.01 nΩ/mG as plotted in Figure 10. The sensitive region is the "donut", the top part of the cavity. Additional tests done showed a greater sensitivity to transverse magnetic field.
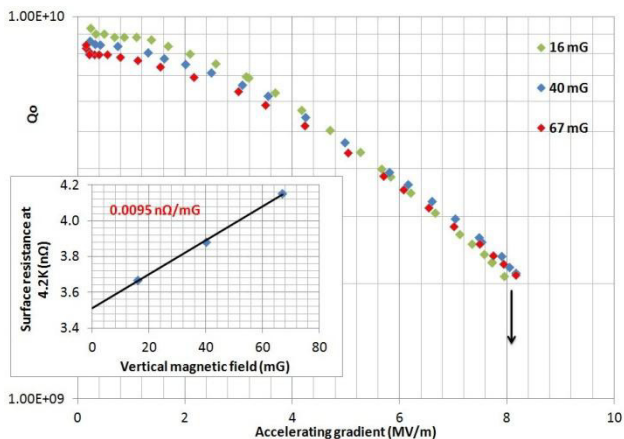
Figure 10: Q_0 curves of a Spiral2 QWR cooled down under three different vertical magnetic configurations (16 mG, 40 mG and 67 mG) at 4.2K

Effect of Cooling Speed Through Transition

Contrary to what has been announced on elliptical cavities; no effect of the cooling speed has been observed as plotted in Figure 11.
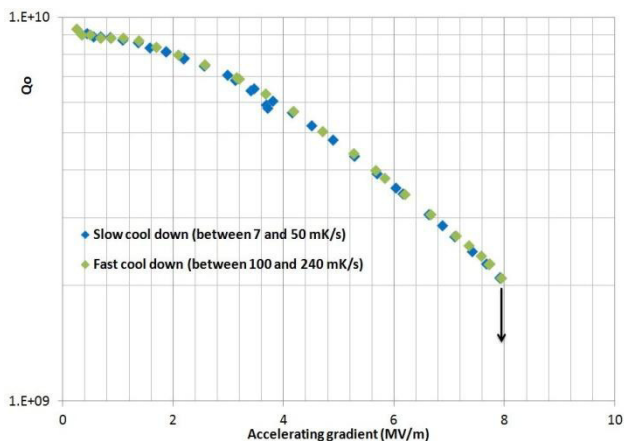

Figure 11: Q_0 curves of a Spiral2 QWR going through transition at two different speeds. No change is measureable.

ESS SPOKE RESULTS

Three Double Spoke Resonators (DSR) have been designed by IPNO [10] and fabricated by two different companies (see Figure 12). These are made of bulk Niobium and will operate at 352 MHz at an accelerating gradient of 9 MV/m with an RF duty cycle of about 5% [11]. Cryogenic losses have to be below 5W.
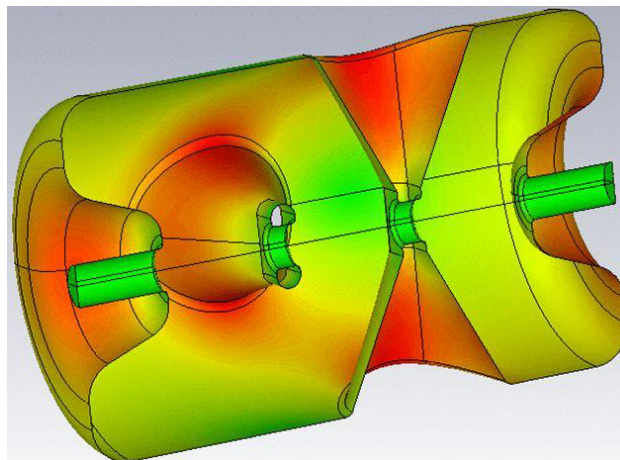

Figure 12: ESS Double Spoke Resonator (DSR).

Analysis of Cavity Results

The three DSR prototypes fabricated already meet the specifications without any particular surface treatment as depicted on Figure 13. They have been prepared following the same procedures; ultrasonic degreasing, 200 μm BCP etching, High Pressure Rinsing and drying in ISO-4 clean-room.
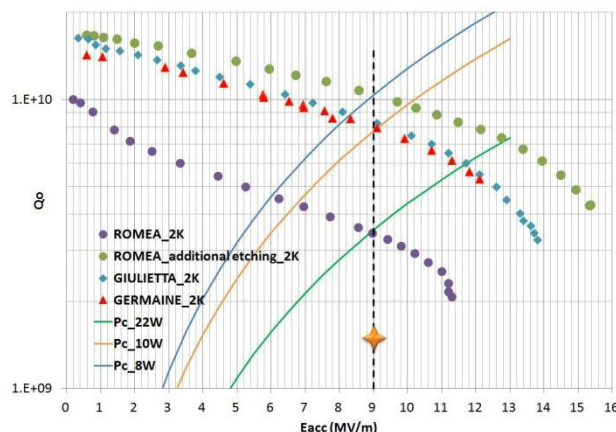

Figure 13: Q_0 curves at 2K of the three DSR prototypes for ESS project.

The very first test of the DSR named ROMEA has showed a very pronounced Q_0-slope (purple circle in Figure 13). This has been attributed to a temperature rise up to 30°C during the etching process leading to a strong hydrogen contamination. Additional etching have been performed (about 60 additional microns kept under 18°C) leading to a nice improvement of the cavity performances (See green circle Figure 13).
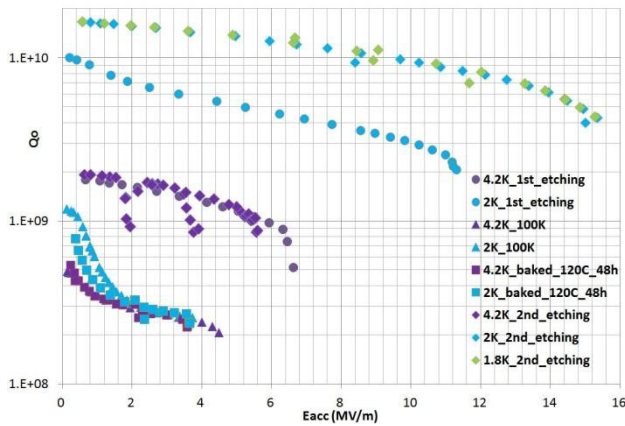
Figure 14: Q_0 curves at 4.2K and 2K of ROMEA DSR.

A first attempt of 120°C baking has been done as shown on Figure 14. Performances were seriously degraded (squares in figure 14) and look like a Q-diseased cavity very similar to the Q-disease test done previously (triangles in Figure 14). The first thought was that the cavity didn't recover from Q-disease test even though the cavity was heated up to 120°C. This scenario has been ruled out thanks to additional tests on Germaine DSR which fully recovers from a Q-disease test after a 300K temperature cycle.

Table 3: Resistances and Model Parameters for a DSR

	Bad etching	**Good etching**	**Q-disease**
Comments	200 μm with T<30°C	Additional 60 μm with T<18°C	6h at 90K
Marker in Figure 13	Circles	Diamonds	Triangles
R_{BCS} at B=0 below 2K	1.5 nΩ	1.5 nΩ	1.5 nΩ
Rres at B=0	11.5 nΩ	6.2 nΩ	100 nΩ
α	6	0.5	>25
γ	2.5	3.4	?
Rres*α (nΩ)	69	3.1	>2500
Rres*γ^2 (nΩ)	71.9	71.7	?

Because of the cryogenic test configuration and space restrictions, these cavities couldn't be tested horizontally as they are supposed to operate, but vertically. This induced a reduction of the cooling efficiency around the beam tube at the bottom especially in non superfluid helium. It has been noticed that above 4 MV/m, the Q_0

was slowly dropping with time. In superfluid helium, the Q_0 was stable up to the maximum accelerating gradient.

As a consequence, the surface resistance model presented previously has only been applied to results of ROMEA DSR in the residual regime below 2K as summarized in table 3. This regime is already reached at 2K (see in Figure 14) as the Q_0 curves at 2K and 1.8K are perfectly superimposed.

Firstly, contrary to Spiral2 QWR, the α parameter, indicating a linear dependence of the residual resistance versus accelerating gradient, is not kept to zero. This linear dependence is typical of a cavity strongly polluted by hydrogen. Indeed, Rres*α is equal to 69 nΩ for the badly etched cavity whereas an additional good etching would make Rres*α drop down to 3.1 nΩ.

Secondly, the Rres*γ^2 is kept constant whatever the quality of the etching. This contribution to the residual resistance is not yet understood. It might be linked to some pollution other than hydrogen as apparently baking a Spiral2 QWR makes it change (see table 2).

Magnetic Behaviour During Cooling-Down

As presented for Spiral2 QWR, the ambient magnetic field is recorded during cooling down to track potential thermal currents or magnetic pollution. Unfortunately, the helium tank welded on the cavity makes the installation of magnetic sensors inside the spokes impossible. Nevertheless, sensors have been positioned around the cavity showing the creation of thermal currents on the bottom of the cavity (see Figure 15). The other sensors (MAG1V+H and MAG2 V+H) didn't show any significant changes. The magnetic field created is maximum during the cooling down when the top of the cavity is still warm and the bottom already around 100K. When approaching the transition, thermal gradients are small and so the magnetic field which is back close to the initial values.
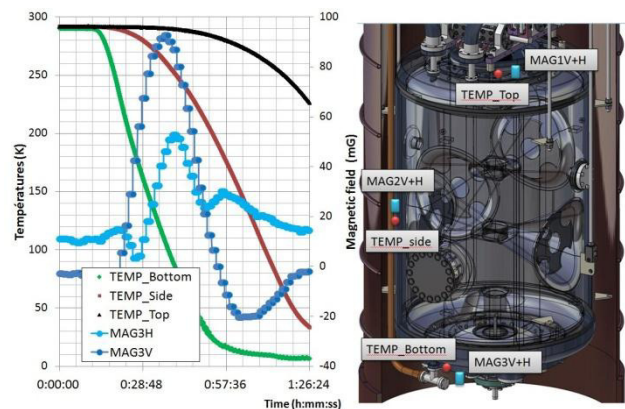

Figure 15: Temperature and magnetic field during cooling down of ESS DSR.

Magnetic Sensitivity ESS DSR

A test has been done to measure the magnetic sensitivity of the ESS DSR in the beam axis direction. The cavity has been tested at 2K with two different

magnetic configuration of the cryostat: Low and 85 mG residual magnetic field (see Figure 16).
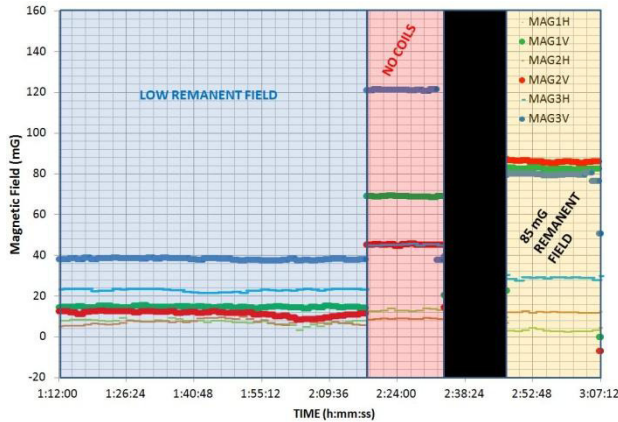

Figure 16: Magnetic field measured in the cryostat at 300K for three different magnetic configurations: Low residual field (optimized to ensure lowest residual field), no coils (active shielding is disabled) and 85 mG vertical residual field (horizontal components stay low).

The analysis of the Q_0 curves at 2K (residual regime) thanks to the model presented earlier is showing that the residual resistance is increased of 5 nΩ for a vertical magnetic field increased of 62 mG (Figure 17). The sensitivity of the DSR to a magnetic field parallel to the beam axis is then of 0.08 nΩ/mG.
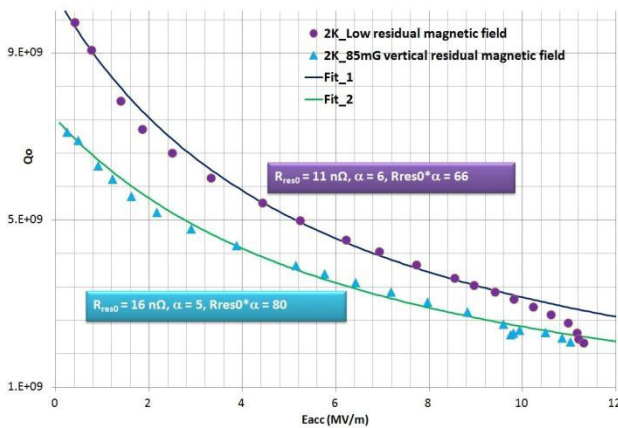

Figure 17: Q_0 curves of an ESS DSR tested at 2K and cooled down through transition in two different magnetic field configurations.

CONCLUSION

As a conclusion, many interesting results have been found on SPIRAL2 Quarter-Wave-Resonator and ESS Double-Spoke-Resonator especially about the magnetic behaviour during cooling down. The accessibility of some key positions (inside the spoke bar for ESS DSR for example) is limited. The analysis is then difficult and requires additional tests to find the best positions in a specific geometry for magnetic sensors. Magnetic measurements are now done routinely to ensure that a bad Q_0 is not due to a magnetic pollution or to important

thermal currents. Improvements of the active (coils) and passive (mu-metal) magnetic shielding are being done to have a better homogeneity of the vertical and horizontal residual magnetic field and thus more confident results on its real effect on the Q_0.

The surface resistance model presented gives very satisfactory agreements and has been upgraded; another simulation code has been used with the capability of exporting surface fields associated to the mesh surface area instead of assuming a constant mesh size as done in [2]. The physical meanings of α, γ and β parameters have been addressed. α and γ are clearly material dependent whereas β is a correction factor for discrepancy between the modelled and the real geometry.

ACKNOWLEDGMENT

REFERENCES

[1] A. Romanenko et al., "Dependence of the Microwave Surface Resistance of Superconducting Niobium on the Magnitude of the RF Field". Applied Physics Letters 102, 252603 (2013).

[2] D. Longuevergne et al., "Magnetic Dependence of the Energy Gap: a Good Model to Fit Q-slope of Low Beta Xavities", Proceedings of the 16th International Conference on RF Superconductivity, SRF'13, Paris, France (2013).

[3] A. Grassellino, "Q-Slope Analysis of Low-Beta SRF Cavities", AIP Conference Proceedings 1352, 161.

[4] G. Ciovati, "High Q at low and medium field" in Proceedings of Argonne Workshop 24th, 2004.

[5] G. Olry, "development of a beta 0.12, 88 mhz, quarter wave resonator and its cryomodule for the spiral2 project," proc. of 12th International Workshop on RF Superconductivity, Ithaca, 2005.

[6] B. Visentin, "Q-slope at high gradients:review of experiments and theories", proc. of 11th International Workshop on RF Superconductivity, Lübeck, 2003.

[7] B. Visentin, "Change of RF Superconductivity Parameters Induced by Heat Treatment on Niobium Cavities", proc. of 10th International Workshop on RF Superconductivity, Chicago, 2001.

[8] J.Halbritter, "Comparison Between Measured and Calculated RF Losses in the Superconducting State" Z.Phys. 238, 466 (1970).

[9] M. Fouaidy, "Detectors Sensing Second Events Induced by Thermal Quenches of SRF Cavities in He II", MOPB023, SRF2015, Whistler, Canada.

[10] P. Duchesne, "Design of the 352 Mhz, Beta 0.50, Double-Spoke Cavity for ESS", Proceedings of the 16th International Conference on RF Superconductivity, SRF'13, Paris, France (2013).

[11] ESS Accelerator TDR. Website : https://europeanspallationsource.se/accelerator-documents